

Elusive Unfoldability: Learning a Contact Potential to Fold Crambin

Michele Vendruscolo and Eytan Domany

Department of Physics of Complex Systems, Weizmann Institute of Science, Rehovot 76100, Israel

We investigate the extent to which the commonly used standard pairwise contact potential can be used to identify the native fold of a protein. Ideally one would hope that a *universal* energy function exists, for which the native folds of *all* proteins are the respective ground states. Here we pose a much more restricted question: is it possible to find a set of contact parameters for which the energy of the native contact map of a *single protein* (crambin) is lower than that of all possible physically realizable decoy maps. We seek such a set of parameters by *perceptron learning*, a procedure which is guaranteed to find such a set if it exists. We found that it is extremely hard (and most probably, impossible) to fine tune contact parameters that will assign all alternative conformations higher energy than that of the native map. This finding clearly indicates that it is impossible to derive a general pairwise contact potential that can be used to fold any given protein. Inclusion of additional energy terms, such as hydrophobic (solvation), hydrogen bond or multi-body interactions may help to attain foldability within specific structural families.

Keywords: protein folding; protein folding potential; contact map; neural networks; perceptron.

I. INTRODUCTION

Nearly all the important biochemical tasks of organisms such as catalytic activity, molecular recognition and transmission of signals are performed by proteins [1]. The biological function of these macromolecules is determined by the specific shapes into which they fold under physiological conditions. The blueprint for the protein's conformation is its chemical composition, e.g. amino acid sequence. The central problem of *protein folding* [1] is to predict proteins' native structures from their amino acid sequences; solution of this problem will have a formidable impact on molecular biophysics and drug design. At present, genome projects have made available the sequences of hundreds of thousands of proteins [2]. The full potential of this achievement will be realized only when we are able to routinely translate the knowledge of a sequence of a protein into the prediction of its shape and function. Moreover, since by using powerful recombinant DNA techniques [3] we can now create proteins with any pre-designed amino acids sequence, it will be possible to create synthetic proteins with entirely novel functions.

A conceptually straightforward attempt to solve the problem is to construct, for any given molecule, an energy function using the inter-atomic potentials and look for energy minima. Alternatively, one can use molecular dynamics, e.g. work at an energy cor-

responding to kT and integrate Newton's equations. Such a direct attack on the problem lies beyond the possibilities of existing computers, partly because of the large number of atoms that comprise a single protein and partly because the exact potential is not known (we are looking for a classical effective interaction between ions and atoms; furthermore, folding takes place in the presence of water and the water molecules must be "integrated out"). This state of affairs points to a need for approximate, coarse grained or reduced representations of protein structure and derivation of corresponding energy functions.

A minimalistic representation of a protein's structure is given by its *contact map* [4–8]. The contact map of a protein with N residues is a $N \times N$ matrix \mathbf{S} , whose elements are defined as

$$S_{ij} = \begin{cases} 1 & \text{if residues } i \text{ and } j \text{ are in contact} \\ 0 & \text{otherwise} \end{cases} \quad (1)$$

One can define contact between two residues in different ways. In this work, we will consider two amino acids in contact when their two C_α atoms are closer than 8.5 Å [8]. Given all the inter-residue contacts or even a subset of them, it is possible to reconstruct quite well a protein's structure, by means of either distance geometry [9], Molecular Dynamics [10] or Monte Carlo [8].

In contrast to Cartesian coordinates, the map representation of protein structure is independent of the coordinate frame. This property made contact maps attractive for protein structure comparisons and for *searching a limited database* for similar structures [4–6]. A more challenging possibility was proposed recently [7]: to use the contact map representation for *folding, e.g. to search the space of contact maps* for the map that corresponds to the native fold. The central premise of this program is that the contact map representation has an important computational advantage; changing a few contacts in a map induces rather significant large-scale coherent moves of the corresponding polypeptide chain [11]. The proposed program faces, however, three considerable difficulties:

1. One needs an efficient procedure to execute these non-local moves
2. There must be a way to test that the resulting maps correspond to physically realizable conformations and
3. One should construct a reliable (free) energy function, defined in contact map space, such that low-energy maps can be used to identify the native one.

We made considerable progress [11] on the first of these problems and have found an efficient method to solve the second [8]. In this study we present some new questions that are relevant to the third issue, of identifying a reliable energy function. We also introduce a suitable methodology to address the questions raised.

The most commonly used energy function for threading sequence \mathbf{a} into a fold whose contact map is \mathbf{S} has the form

$$E(\mathbf{a}, \mathbf{S}, \mathbf{w}) = \sum_{ij} S_{ij} w(a_i, a_j). \quad (2)$$

The 210 parameters $w(a_i, a_j)$ represent the energy gained by bringing amino acids a_i and a_j in contact.

Of the two main methods that have been used in the past to derive contact energy parameters, knowledge-based techniques were the first to be proposed. These methods rely on the quasi-chemical approximation [12–16] to derive contact energies from a statistical analysis of known protein structures. Although suitable for more limited purposes, such as fold recognition [17] or threading [12], energy parameters obtained this way have failed, so far, to produce acceptable maps by energy minimization (sometimes referred to as *ab initio* folding).

More recently, much attention has been devoted to a new class of potentials, derived by optimization [18–23]. For example Mirny and Shakhnovich [22] determine the contact energy parameters by minimizing simultaneously the Z-score of the native maps of a large set of proteins. Hao and Scheraga [20], using a much more detailed representation, tried to find energy parameters for which the native conformation has the lowest energy for a single protein.

In this work we address the same problem as Hao and Scheraga, but use the contact representation. That is, we ask whether *it is possible to find contact energy parameters, such that among all physical maps for a particular it single protein, the energy of the native map is the lowest?* In more detail, one requires that

$$E(\mathbf{a}, \mathbf{S}_0, \mathbf{w}) < E(\mathbf{a}, \mathbf{S}_c, \mathbf{w}). \quad (3)$$

That is, the parameters \mathbf{w} should be such that when the sequence \mathbf{a} is threaded into *any* physical non-native contact map \mathbf{S}_c , the resulting energy should be higher than that of the native map \mathbf{S}_0 .

Asking the question posed above in the contact energy representation has a distinct advantage over other potentials, since in our case the energy is a *linear function* of the parameters \mathbf{w} . Therefore once a large library of candidate maps \mathbf{S}_c has been generated, one can search, by the well known method [24–28] of *perceptron learning*, for a set of \mathbf{w} for which Eq.(3) holds for *all* maps from this library.

Even though ideally Eq.(3) should be satisfied for any sequence \mathbf{a} of amino acids, existing in nature or synthesized, it is not clear at all that it is possible to find a set \mathbf{w} for which (3) holds for even a single protein. The reason is that as we have recently shown [29], the number of physically realizable contact maps is exponential in the length N of the protein¹. Thus for a short protein (with, say, $N = 40$), Eq.(3) implies that about 2^{40} conditions should be satisfied by tuning 210 parameters!

We believe that this is a highly relevant question; clearly the true potential (which, of course, is far more complex than our Eq (2)) is able to fold all natural proteins: there should be a potential of intermediate complexity between the true one and the simple contact energy we are testing here, which is able to fold, say, a family of proteins. This work is a

¹The number of self avoiding walk configurations is also exponential, albeit with a larger coefficient of N in the exponent

first step towards developing a methodology to test any such potential.

It is important to realize that the conditions we try to satisfy are much more stringent than the one usually required for successful *threading* [17,30,31]. We did succeed [32] to find a set of contact energies \mathbf{w} that satisfies Eq.(3) simultaneously for a large family of proteins, provided the decoy maps \mathbf{S}_c were obtained by (gapless) threading. The reason is that a contact map obtained by threading is, usually, a rather poor guess for the native fold [17,30,31] (see Fig. 1 of energy histograms of threading and minimization).

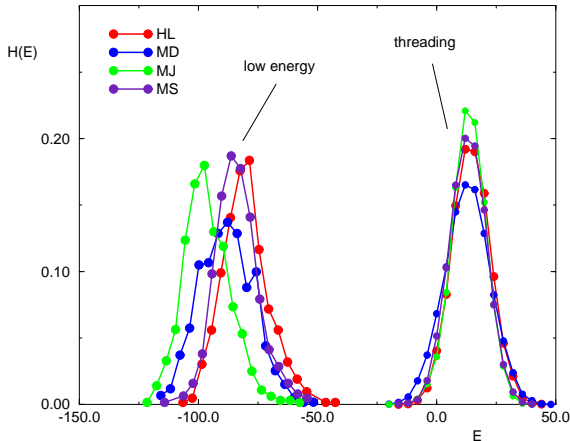


FIG. 1. Histograms that demonstrate the difference in energy between ensembles of contact maps obtained by threading and by energy minimization. We used 4 sets of contact energy parameters: HL, Hinds and Levitt [13]; MD, Mirny and Domany [7]; MJ, Miyazawa and Jernigan [12]; MS, Mirny and Shakhnovich [22].

Since one cannot perform an exhaustive search of all physical maps, we must *generate* a large ensemble of alternative contact maps of low energy. We will assume that only such a subset of contact maps is effectively in competition with the native one to be the ground state and only these maps gives rise to relevant constraints in Eq.(3).

Our strategy and the outline of this paper are as follows:

- *Generation of alternative conformations:* in Sec II we outline briefly the manner in which such a set of low-energy alternatives is generated. Details of this method will be presented in a separate publication [11].

- *Learning of a set of pairwise contact energy parameters:* in Sec. III, we present the way in which we use these contact maps to “learn” the energy parameters; the results obtained for a single protein, crambin, are in Sec IV.
- Our results are summarized in Sec V, where we also discuss perspectives and future directions.

We chose crambin as the particular protein to study since it has a long standing history in protein folding simulation investigations. Wilson and Doniach [33] used a simplified model in which the conformation of the backbone and side chains is specified by dihedral angles and contact energies are calculated from the distribution of pairwise distances observed in known experimental structures. Among other results, they were able to correctly reproduce the formation of secondary structures and many of the features of the hydrophobic core. Kolinski and Skolnick [34] performed accurate Monte Carlo simulations using a detailed lattice representation, optimized for the prediction of helical proteins. In their model, side chain rotamers were explicitly represented by additional single monomers. The energy function, mostly of statistical origin, contained several terms to help the cooperative assembly of secondary structures and the packing of the side chains. On average, their simulation runs ended up in conformations with the correct topology of the native fold, and a RMSD distance of 3 Å from the native C_α trace. Hao and Scheraga [20,21] showed, by optimizing an extended set of energy parameters, that it is possible to fold crambin within 1-2 Å RMSD from the native state. Their conclusion is, however, that it is always possible to find structures with lower energy than the native state.

It should be borne in mind that within the contact map representation, conformational fluctuations, as measured by RMSD, amount to 1.1 Å for crambin. This result is obtained by constructing 1000 structures, following the method described in Ref. [8], all with contact maps *identical* to the native one, and averaging their RMSD values.

Within the contact energy model, existing sets of contact potentials perform very poorly in a computer experiment of folding crambin. We demonstrated this by performing a Monte Carlo minimization, using these potentials, starting from the experimentally known native structure. For all the contact potentials tested this procedure identifies easily conformations that are very different from the native one, and of significantly lower energy (see Fig. 1). This clearly proves that for these potentials en-

ergy minimization will lead to non-native states and also demonstrates that our minimization procedure yields maps of much lower energy than those obtained by threading.

II. GENERATION OF ALTERNATIVE CONFORMATIONS

Crambin [36] is a protein of length $N = 46$; its native map, constructed by taking the coordinates of the C_α atoms from the PDB and using a threshold of 8.5 Å to define contacts, is shown in Fig.2.

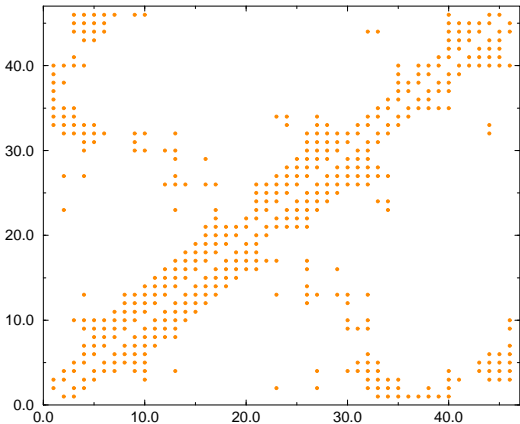


FIG. 2. Contact map for the native state of crambin. Dark dots represent contacts ($S_{ij} = 1$). There are 187 non-nearest neighbors contacts.

Our aim is to generate maps of energy low enough to “compete” with the native contact map. These alternative candidate maps should be markedly different from one another, e.g. have a large relative Hamming distance [8]

$$D^{\text{map}} = \sum_{j>i} |S_{ij} - S'_{ij}|. \quad (4)$$

The number of contact maps that can be actually sampled in any reasonable time is a negligible fraction of the $O(e^{46})$ physical maps. Therefore, moving in an efficient way in the space of physical contact maps is an essential component of our program. Clearly, by turning existing contacts off and non-existing ones on, we can generate large scale moves of the polypeptide chain; moves that would have taken very long time to accomplish in real space. This is

one of the most attractive features of working with contact maps. There are two main problems with doing this. First, if one selects at random the contacts that are to be modified, chances are that the resulting maps will not be physical [7]: that is, there exists no real polypeptide chain conformation whose contact map is the one we found. The second problem is that we would like to work with moves that do not destroy secondary structure elements (α -helices and β -sheets).

As can be seen from Fig.2, these appear as clusters of non-zero entries in the map. Thick bands along the principal diagonal represent α helices; the small antiparallel β sheet which characterizes the native fold of crambin appears as a thick band, perpendicular to the principal diagonal, whose two strands extend from amino acids 1 to 4 and from 32 to 35, respectively. A contact map is roughly characterized by the number and the respective positions of its secondary structure elements. A typical native map has, in addition, isolated entries (single contacts or small clusters) that contain information about the global fold and relative positions of the secondary structure elements.

We present here only a short description of our Monte Carlo method; for a more detailed exposition we refer the reader to Ref. [11]. Our algorithm consists of three steps. The first step consists of *non-local moves*. We start by identifying “clusters” of contacts in an existing map. These clusters represent either α -helices or β -sheets (parallel or anti parallel), or small groups of contacts between amino acids that are well-separated along the chain. The clusters are identified on a given map by laying down bonds that connect neighboring contacts on the map and identifying clusters of contacts that are connected by such bonds [11]. Some of the existing clusters of contacts are removed and some other groups are restored elsewhere. This way secondary structure elements are destroyed and recreated at different locations and orientations. The “energy” of the resulting coarse map is evaluated and a low energy map is retained. This map serves as the starting point for the second step: *local moves*. This is a refinement procedure that consists of turning on or off (mostly one at a time) contacts that are in the vicinity of existing ones, following some of the rules introduced in Ref. [7]. Again, only moves that lower (or do not significantly raise) the energy are accepted. These first two steps are fast operations, since they involve binary variables. Most of the computer time is taken by the third step, *reconstruction*, where we deal with the major problem of ensuring

that we stay in the subspace of physical maps.

A generic contact map is not guaranteed to correspond to any real conformation of a polypeptide chain in space. To solve this problem, we developed an efficient Monte Carlo reconstruction method that checks whether any given target map is physical or not [8]. This is done by working with a string of beads that represents the backbone of the polypeptide chain. The beads are moved around without tearing the chain and without allowing one bead to invade the space of another. The motion of this string is controlled by a “cost function” which vanishes when the contact map of the string coincides with that of the target map. The cost increases when the difference between the two maps increases. This procedure ends up with a chain configuration whose contact map is physical by definition and close to the target map. Thus we are able to efficiently “project” any map that we have generated in the first two steps onto the subspace of physical maps.

Having described the manner in which a single low energy chain and its corresponding map are obtained, we turn to describe the manner in which we generated a representative ensemble of contact maps, to be used in the derivation of contact energy parameters. In general, one expects to have two interplaying levels of optimization. On the one hand, one has to satisfy Eq.(3) for contact maps that are very different from the native one. On the other hand, with the same set of energy parameters, one should be able to discriminate between the native contact map and those maps that are close to it. We generated conformations close to the native one by running a series of Monte Carlo minimizations, *starting from the native state*. This procedure was *not* carried out in contact map space, but rather by using a local Monte Carlo procedure on the backbone or chain of beads described above, with the position of each bead defined in real space; the elementary move of this procedure is of the crankshaft type [35]. Each minimization consist of N_{LMC} such Monte Carlo steps and yields a chain and its low-energy candidate contact map. A move is accepted according to the Metropolis prescription at a given fictitious temperature T_{LMC} . The procedure is then repeated, starting again from the native state but using different random numbers and generating a different map. We call this procedure D_1 ; it generates an ensemble of low energy maps that are (relatively) close to the native fold.

To generate conformations far from the native one, we use the three-step Monte Carlo method described above, supplemented by a fourth step; a further real

space Monte Carlo minimization, as in procedure D_1 . That is, the three-step algorithm that performs global moves in contact map space ends with a chain conformation; this is used as the initial state of the D_1 procedure (again using N_{LMC} local steps). Each search gives rise to a low energy contact map. Such a contact map is used as the starting point for the following global search. This second procedure, called D_2 , generates a set of low energy maps that are very different from the native fold. In Fig. 3 we show energy versus Hamming distance of typical contact maps obtained by procedures D_1 and D_2 .

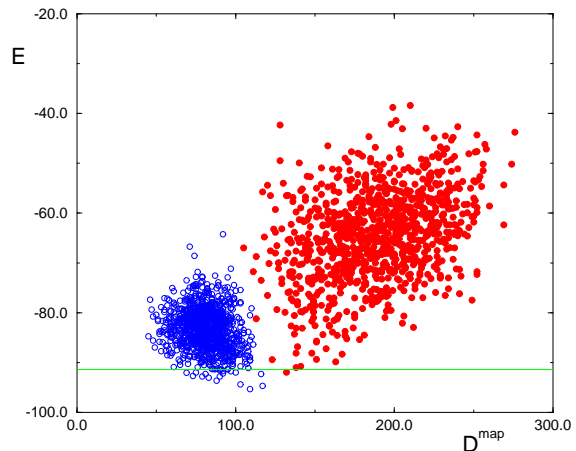


FIG. 3. Energy E versus Hamming distance D^{map} for 1000 contact maps obtained by procedures D_1 and D_2 . The contact maps are generated using the energy parameters of epoch $t = 9$ (see next section) and $N_{LMC} = 10^6$. The line corresponds to the energy of the native contact map of crambin.

The energies and maps obtained by the two minimization procedures depend strongly on the length of the run. As a part of our strategy, we repeated procedures D_1 and D_2 for $N_{LMC} = 10^3, 10^4, 10^5, 10^6, 10^7$ local steps. By combining the two sets of contact maps derived by the two minimization procedures, we obtained a representative set of P contact maps.

III. LEARNING CONTACT ENERGIES

A. Derivation of contact energies as a learning problem

In the crambin [36] chain, 5 out of the 20 amino acids do not appear and 3 appear only once. Thus, among the corresponding 210 possible contact energies, only 117 parameters can effectively enter the energy (2) for any set of candidate maps. These parameters form a 117-component vector \mathbf{w} . The native map of Fig.2 contains 187 non-nearest neighbor contacts, which involve only 72 of the 117 possible contact energy parameters. We now show that for any map \mathbf{S}_μ the condition Eq.(3) can be trivially expressed as

$$\mathbf{w} \cdot \mathbf{x}_\mu > 0 \quad (5)$$

To see this just note that for any map \mathbf{S}_μ the energy (2) is a linear function of the 117 contact energies that can appear and it can be written as

$$E(\mathbf{a}, \mathbf{S}_\mu, \mathbf{w}) = \sum_{c=1}^{117} N_c(\mathbf{S}_\mu) w_c \quad (6)$$

Here the index $c = 1, 2, \dots, 117$ labels the different contacts that can appear and $N_c(\mathbf{S}_\mu)$ is the total number of contacts of type c that actually appear in map \mathbf{S}_μ . The difference between the energy of this map and the native one is therefore

$$\Delta E_\mu = \sum_{c=1}^{117} x_c^\mu w_c = \mathbf{w} \cdot \mathbf{x}_\mu \quad (7)$$

where we used the notation

$$x_c^\mu = N_c(\mathbf{S}_\mu) - N_c(\mathbf{S}_0) \quad (8)$$

and \mathbf{S}_0 is the native map.

Each candidate map \mathbf{S}_μ is represented by a vector \mathbf{x}_μ and hence the question raised in the introduction becomes whether one can find a vector \mathbf{w} such that condition (5) holds for all \mathbf{x}_μ ? If such a \mathbf{w} exists, it can be found by *perceptron learning*.

B. Perceptron: Learning from examples

A perceptron is the simplest neural network [24]. It is aimed to solve the following task. Given P patterns (also called input vectors, examples) \mathbf{x}_μ , find a vector \mathbf{w} of weights, such that the condition

$$h_\mu = \mathbf{w} \cdot \mathbf{x}_\mu > 0 \quad (9)$$

is satisfied for every example from a training set of P patterns, \mathbf{x}_μ , $\mu = 1, \dots, P$. If such a \mathbf{w} exists for the training set, the problem is *learnable*; if not, it is *unlearnable*. We assume that the vector of “weights” \mathbf{w} , as well as all examples \mathbf{x}_μ are normalized,

$$\mathbf{w} \cdot \mathbf{w} = \mathbf{x}_\mu \cdot \mathbf{x}_\mu = 1 \quad (10)$$

The vector \mathbf{w} is “learned” in the course of a training session. The P patterns are presented cyclically; after presentation of pattern μ the weights \mathbf{w} are updated according to the following learning rule:

$$\mathbf{w}' = \begin{cases} \frac{\mathbf{w} + \eta \mathbf{x}_\mu}{|\mathbf{w} + \eta \mathbf{x}_\mu|} & \text{if } \mathbf{w} \cdot \mathbf{x}_\mu < 0 \\ \mathbf{w} & \text{otherwise} \end{cases} \quad (11)$$

This procedure is called learning since when the present \mathbf{w} misses the correct “answer” $h_\mu > 0$ for example μ , all weights are modified in a manner that reduces the error. No matter what initial guess for the \mathbf{w} one takes, a convergence theorem guarantees that if a solution \mathbf{w} exists, it will be found in a finite number of training steps. [24,25].

Different choices are possible for the parameter η . Here we use the learning rule introduced in Ref. [28], since it allows, at least in principle, to assess whether the problem is learnable. The parameter η is given at each learning step by

$$\eta = \frac{-h_\mu + 1/d}{1 - h_\mu/d} \quad (12)$$

where the parameter d (called despair) evolves during learning according to

$$d' = \frac{d + \eta}{\sqrt{1 + 2\eta h_\mu + \eta^2}}. \quad (13)$$

Initially one sets $d = 1$.

The training session can terminate with only two possible outcomes. Either a solution is found (that is, no pattern that violates condition (9) is found in a cycle), or unlearnability is detected. The problem is *unlearnable* if the despair parameter d exceeds a critical threshold [28]

$$d > d_c = \frac{M^{M+1}}{2^{M-1}}, \quad (14)$$

where M is the number of components of \mathbf{w} .

Evidently, once the requirement posed in the introduction, Eq (3), has been expressed in the form (5), the question whether it does or does not have a

solution reduces to deciding whether a set of examples is learnable by a perceptron. Every candidate contact map (generated by the search procedure described above) provides a pattern for the training session. Note that the vector \mathbf{x} defined in Eq. (8) must be normalized before (11) is used. Before turning to present our results for the learnability of crambin using $M = 117$ contact parameters, we address the same question but use a much simpler potential, that of the HP model [37]

C. Can the HP model stabilize crambin?

We tried to stabilize the native map of crambin using the parametrization of the HP model. This has an even simpler potential than the one we use; whereas we have 117 contact energies to tune, the HP model attempts to satisfy Eq. (3) using only $M = 3$ parameters, w_1, w_2, w_3 . The perceptron learning procedure detected clearly and unambiguously that this is an unlearnable problem.

We relabeled the amino acids in the crambin sequence following the usual partition into hydrophobic (H) and polar (P) residues. Examples were generated and then the perceptron learning procedure was applied to this problem. We measured the value of the despair d as learning progressed; the result is shown in Fig. 4. The critical value $d_c = 3^4/2^2$ was reached rather fast when we used only 306 examples; that is, we established that the problem is unlearnable.

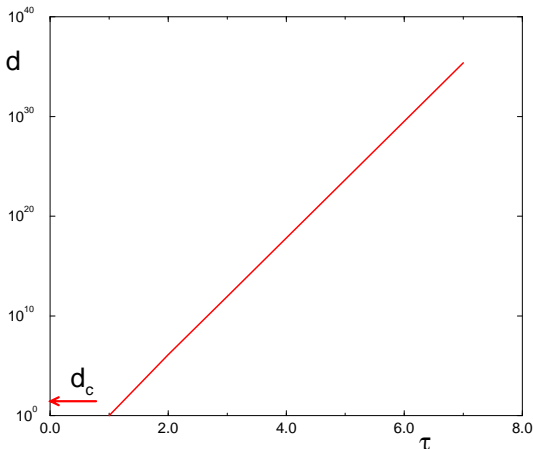


FIG. 4. Increase of the despair d with the number τ of learning sweeps for the HP learning.

This is a very important lesson from a simple model: with only 2 species of amino acids, the contact map representation is not suitable for folding crambin since it is *impossible* to find a set of contact energy parameters that satisfy Eq.(3). We regard the present work, which employs contact energy parameters between the 20 existing species of amino acids (15 for crambin), as the first step in a progressive and controlled improvement of protein structure representation.

The question we posed concerns learnability of an exponential number of examples, of which we can sample only a small subset. When 15 amino acids are used the problem is far from being as simple as the HP model; this is evident from the fact that a large number of examples, generated by threading, can be easily learned. Hence, in order to answer the question we posed it is important to choose a strategy that generates “hard” examples. Such a strategy is described next.

D. Iterative Learning and Generation of Examples

The contact energy parameters are learned in an iterative manner, i.e. examples are generated and then learned; the new \mathbf{w} is then used to generate new examples and so on. We will refer to each such iteration as an *epoch*. At epoch $t = 0$ we start from an arbitrary set \mathbf{w}_0 of parameters; we used those that were derived in Ref. [8] for the present C_α representation. Using the procedure of generation of low energy conformations discussed above with these energy parameters, we generated a set of P_0 low energy contact maps. This completes epoch 0 and we can start epoch $t = 1$. The P_0 low energy contact maps obtained in epoch 0 constitute the training set to learn new contact parameters, \mathbf{w}_1 , according to the perceptron learning rule discussed in the previous section. Using the newly derived energy parameters, we generate a new set of P_1 low energy contact maps. This set is added to the old training set so that now we have $P_0 + P_1$ examples, all of which are learned in epoch $t = 2$. In the present work this iterative procedure is repeated up to epoch 10.

IV. ELUSIVE UNLEARNABILITY

A. Impracticality of despair

We summarize here our main result about the question we have addressed in the present work. We will present below considerable evidence supporting our main conclusion:

the problem of fine tuning the contact energy parameters to stabilize the native state of crambin is *effectively unsolvable*.

By this we mean that the problem is either unlearnable, or learnable with a learning time which exceeds any realistic scale. We cannot give a clear-cut answer as we did for the HP model since the condition that should be met [28] to establish unlearnability is numerically impractical; according to Eq.(14), for $M = 117$, the critical despair $d_c \simeq 10^{87}$. Moreover, from Fig.5 we see that in this particular problem, when we tried to learn $P = 195124$ examples, the despair d increases *logarithmically* with the learning time τ . This particular learning task took $\tau = 606756$ sweeps to be solved, and the final value of the despair was $d = 4921.01$. The size of P and τP and τ is strikingly larger than those involved in the HP case, where $\tau = 2$ sweeps and $P = 306$ examples were enough to obtain an unambiguously negative answer, (in that case after $\tau = 7$ the despair was $d > 10^{30}$).

This is also in contrast to perceptron learning of $P > 2M$ randomly generated examples (which is an unlearnable problem [26,27] for large M); there d grows *exponentially* with learning time [28]. Since the time that would be needed to exceed the critical despair in our particular problem is beyond any reasonable estimate, we have to resort to alternative non-rigorous ways to test learnability of this task.

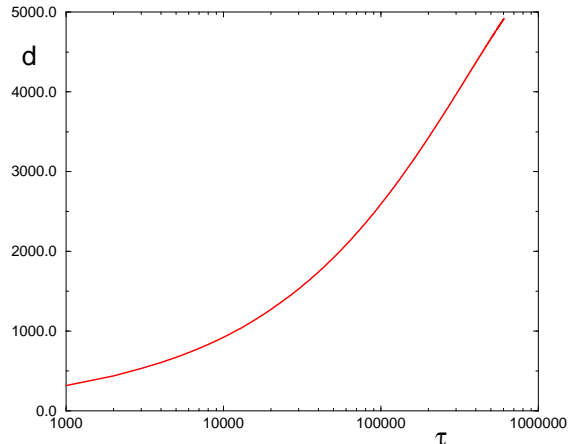


FIG. 5. Increase of the despair d with the number τ of learning sweeps for a typical case of learning dealt with in this work.

B. Generalization error

As explained above, the parameters \mathbf{w} that were obtained after a new epoch solve a larger training set of examples and, hence, they may well be a “better solution” of the problem. The quality of any solution \mathbf{w} is measured by the *generalization error* ε_g . To determine it, one generates a set of new examples that were not used in the training procedure; ε_g is the fraction of examples for which \mathbf{w} produces the wrong answer and it should decrease when the training set is increased.

In the context of our problem we generate at epoch t , using the procedure described above with the current energy parameters \mathbf{w}_t , a set of P_t of low-energy contact maps. $\varepsilon_g(t)$ is the fraction of those contact maps that violate Eq.(3) and hence have lower energy than the native map. The dependence of $\varepsilon_g(t)$ on the epoch index t is shown in Fig. 6.

Initially $\varepsilon_g(t)$ decreases drastically with t . We used several of the existing knowledge-based contact potentials [7,12,13,22] as our starting energy parameters \mathbf{w}_0 ; the fact that $\varepsilon_g(0) \simeq 1$ signals that these potentials fail completely the test of assigning the native map an energy that is lower than that of maps obtained by our minimization procedure. This is to be compared with the good performance of the same potentials on testing the native fold against maps obtained by *threading* [32], highlighting the point made in the Introduction, that stabilizing the native map against our low-energy decoys is a much more dif-

difficult challenge than stabilizing it against maps obtained by threading.

With increasing epoch index, however, the generalization error does not level out at zero; rather, it fluctuates at the level of 0.2 - 1 percent. Complete learning is elusive; this behavior indicates that the problem is, probably, unlearnable.

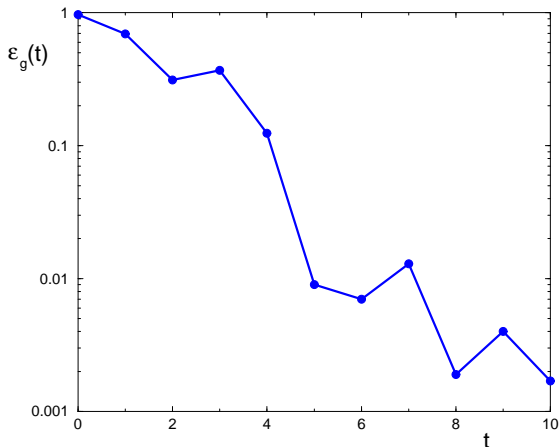


FIG. 6. Generalization error $\epsilon_g(t)$ of conformations with energy lower than the native state as a function of the epoch t .

C. Learning time

Further evidence supporting unlearnability comes from the way the learning time τ increases with the size of the training set. τ is defined as the number of sweeps through the entire training set that is needed to learn all the P examples. In an unlearnable case there exist sets of examples for which no solution can be found; for large enough P the training set will include, with non-vanishing probability, such an unlearnable subset. This means that the learning time τ diverges for a finite P . We show in Fig. 7 the average inverse learning time $1/\langle\tau\rangle$ as a function of the inverse number $1/P$ of examples. The curve was obtained as follows. At the end of our last epoch we collect all P^{tot} contact maps that have been accumulated so far (during all epochs). Of these we randomly select a subset of ΔP maps and compute the learning time τ . This process is repeated N_L times, each time selecting a different set of ΔP examples. $\langle\tau\rangle$ is the average learning time of these N_L learning processes. To study how the learning time τ increases with the number of training examples,

we repeat the previous procedure, randomly selecting N_L training sets of $P = n\Delta P$ patterns in each and compute the average learning time as before. In the data shown in Fig. 7 we used $N_L = 6$ at epoch $t = 9$. We followed this random selection procedure to eliminate all possible dependence of the learning time on the epoch index, isolating the variation of τ with the size of the training set.

The observed increase of the learning time with P is compatible with a divergence of $\langle\tau\rangle$ at some finite $P_c \approx 5 \cdot 10^5$, again indicating unlearnability.

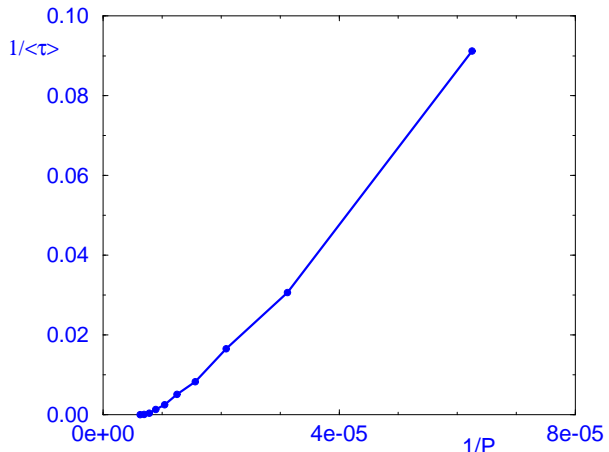


FIG. 7. Inverse average learning time $1/\langle\tau\rangle$ as a function of the inverse number $1/P$ of examples.

V. ANALYSIS OF THE CONTACT ENERGIES

Even though the problem is apparently unlearnable, our procedure produces contact energies that have several appealing features. One of these has been mentioned above: whereas for the existing contact potentials it is very easy to find maps whose energy is below that of the native map, with the \mathbf{w} obtained after several training epochs this becomes a difficult (albeit possible) task (see Fig. 6). That is, the generalization error becomes very small. We present now some other features of the contact parameters obtained by our learning procedure.

A. Energies of the false ground states

Another measure of the quality of the energy parameters is given by the gap ΔE between the ener-

gies of the false ground states and that of the native map. A negative value of ΔE means that (3) is violated.

We found that the average $|\Delta E|$ of the violating examples decreases with the epoch index, see Fig. 8. Hence our learning procedure flattens the energy landscape, reducing both the number of violating examples and their gap. Another relevant question concerns the "location" of these false minima, i.e. how different are the corresponding structures from the native one? To study this, we reconstructed the three dimensional conformations corresponding to the violating examples and measured their average RMSD distance from the native conformation. We found that the RMSD does not decrease with the epoch index; moreover, using procedure D_2 , false minima are found at an approximate average RMSD of 10 Å at *any* epoch. Only their number decreased significantly. Hao and Scheraga [20], on the other hand, reported that the distance of their false ground states from the native conformation did decrease as their energy parameters became better optimized.

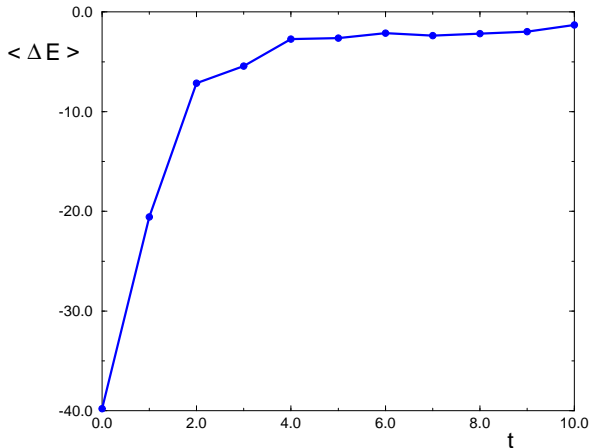


FIG. 8. Energy gap $\langle \Delta E \rangle$ of the violating examples at successive epochs.

B. Energy distribution at successive epochs.

As already observed, with the initial energy parameters the vast majority of the contact maps that are generated have an energy lower than the native contact map. As can be seen from Fig. 9, where the energy scale is shifted so that the native contact map has always zero energy, for increasing epoch index, the energy distribution shifts to the right and

becomes narrower. Learning is thus accompanied by an improvement of the Z -score, which is a commonly used estimator of the quality of a set of energy parameters [22].

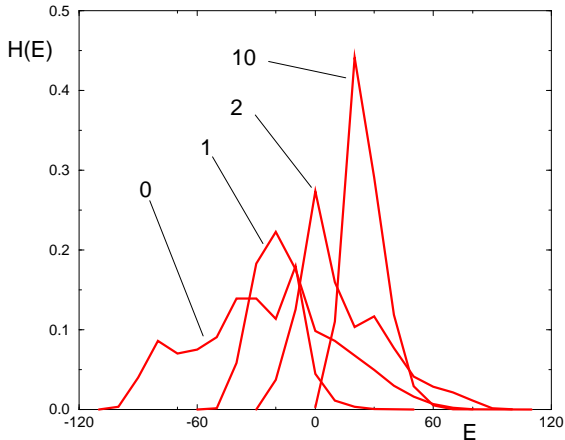


FIG. 9. Normalized histogram $H(E)$ of the energies of the contact maps at epochs $t = 0, 1, 2$ and 10. The energy scale is shifted so that the native contact map energy is 0.

C. Allowed region in parameter space

The vector \mathbf{w} of energy parameters lies on the surface of a unit sphere in the $N_{\mathbf{w}} = 117$ dimensional parameter space. Each example introduces a hyperplane which restricts the allowed vectors to one of its sides. The region which satisfies all the P constraints is called *version space*. All vectors \mathbf{w} that lie within version space are compatible with the constraints given by Eq. (3) and, therefore, are solutions of the learning problem. As more examples are added, version space may shrink - if the problem is unlearnable, the (relative) volume of version space shrinks to zero.

To estimate the size of version space we generated an ensemble of solutions by the following Monte Carlo sampling. At each epoch we arrive by perceptron learning at a particular solution \mathbf{w} that satisfies the set of P examples which define the current version space. Starting from this solution, we performed a random walk on the surface of the unit sphere of \mathbf{w} vectors. The elementary step is to choose at random a component k of \mathbf{w} and to change it,

$$w'_k = w_k + \varepsilon$$

where ε is a random displacement. The new array of weights is kept (and normalized) if it is still a solution, otherwise it is rejected. This updating rule is repeated many times, and eventually a sizeable number of different solutions is obtained. Next we perform a principal component analysis of the covariance matrix of this ensemble of solutions. The covariance matrix is defined as

$$C_{ij} = \langle (w_i - \langle w_i \rangle)(w_j - \langle w_j \rangle) \rangle, \quad (15)$$

where $\langle \cdot \rangle$ denotes averages taken over the ensemble of solutions. Let $\lambda_i > 0$ and \mathbf{v}_i be the eigenvalues and the corresponding eigenvectors of the covariance matrix. Clearly, $\sigma_i = \sqrt{\lambda_i}$ is the standard deviation which measures the spread of our ensemble of solutions \mathbf{w} along direction \mathbf{v}_i . If we observe $\lambda_i \rightarrow 0$, this means that along the corresponding direction the width of version space has shrunk to zero. The projections of our vector of energy parameters along these directions are fixed and cannot be changed. As shown in Fig. 10, the number L of directions whose corresponding eigenvalues approach zero increases with the epoch index t (to about half the number of directions).

We also checked whether the directions that are constrained do or do not change with the epoch index and found that these directions become conserved. The check was performed by measuring for $t > 6$ the variance of the parameters along the directions that were locked at epoch $t = 6$. Hence further optimization of these parameters to fold other proteins is ruled out.

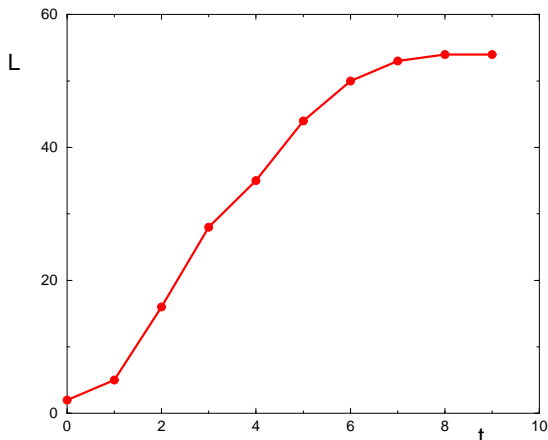


FIG. 10. Number L of locked directions in parameter space as a function of the epoch t .

Another aspect of the solutions derived by learning is their convergence. We calculated, after every epoch t , the *average* solution (i.e. the center of mass of version space), \mathbf{w}_t . The overlap $\Omega = \mathbf{w}_t \cdot \mathbf{w}_{t+1}$ of such average solutions, measured after two successive epochs t and $t + 1$, increases with t to a value very close to 1 (see Fig. 11). This indicates that the vector \mathbf{w}_t converges for large t s to some particular direction.

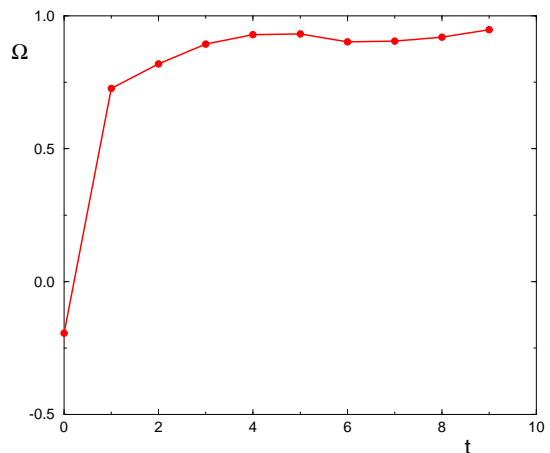


FIG. 11. Convergence of the scalar product $\Omega = \mathbf{w}_t \cdot \mathbf{w}_{t+1}$ in the learning process, as a function of the epoch t .

VI. CONCLUSIONS

One of the simplest and more widely used forms for the energy of a protein is the contact approximation, (see Eq.(2)). Although such approximations have contributed a lot to our understanding of the general properties of the folding transition, it is far from clear which are its intrinsic limitations if the task is to actually predict native conformations from protein sequences.

To give a clear-cut solution to this problem, in this work we have posed a remarkably simple question: Is it possible to optimize a set of contact energy parameters such that the native contact map of a *single* protein has the lowest energy among all the possible alternative contact maps?

We have reached the conclusion that the derivation of an such a set is at the edge of learnability, even in the case of one protein only. For any practical purpose, the basic requirement that the native state of a protein should be the minimum of some

effective free energy, cannot be fulfilled if a contact approximation is used.

We stress the obvious fact that learning a set of contact energy parameters for more than one protein is necessarily more difficult, and would not change our conclusion.

Our conclusion is supported by substantial evidence:

1. If only two species of amino acids are used, the unlearnability of the task is unambiguously shown.
2. When 15 species of amino acids are considered, the time τ needed to learn the set of energy parameters that stabilize crambin increases dramatically with the number P of alternative contact maps that are considered. Such increase of τ is compatible with a divergence at a finite P .
3. The generalization error ε_g does not asymptote to zero, rather it fluctuates around a finite, although small, value.
4. The distance from the native state of contact maps that are found with energy lower than the native one does not decrease as the optimization is carried on.
5. The allowed region in energy parameter space shrinks to zero along roughly a half of the total number of directions. Thus, a further optimization of parameters along these directions is ruled out.

Even within a contact energy framework, more accurate and possibly more successful approximations are possible. For example, an all-atom based definition of contact instead of one based on the C_α only, could be expected to improve the quality of the prediction. We regard, however, the results presented here as a first step towards a systematic improvement of the approximation of the energy function to be used in folding predictions. In planned future work, the simple form of the energy used here will be supplemented with the inclusion of additional energy terms, such as hydrophobic (solvation), hydrogen bond or multi-body interactions.

A different question, which is not in the scope of the present work, is how does a set of contact energy parameters derived by perceptron learning compare with other existing sets. We have addressed this problem by learning together 153 different proteins, and considering alternative conformations generated by gapless threading [32].

This last issue is connected with the possibility to perform predictions that do not rely completely on energy minimization alone. For example, the condition that the native state should be the absolute minimum of the energy function can be relaxed. In such “weak” prediction, a short list of candidates is identified and used as starting point for a successive selection.

This research was supported by grants from the Minerva Foundation, the Germany-Israel Science Foundation (GIF) and by a grant from the Israeli Ministry of Science. We thank Ido Kanter for most helpful discussions.

-
- [1] Creighton, T. E. (ed.), (1992). *Protein folding*, W. H. Freeman and Company, New York.
 - [2] Duboule, D. (1997). The Evolution of Genomics. *Science* **278**, 555, and references therein.
 - [3] Watson, J. D., *et al.*, (1992). *Recombinant DNA*. W. H. Freeman and Company, New York.
 - [4] Chan, H. S. & Dill, K. A. (1990). Origins of structure in globular proteins. *Proc. Natl. Acad. Sci. USA* **87**, 6388-6392.
 - [5] Godzik, A., Skolnik, J. & Kolinski, A. (1993). Regularities in interaction patterns of globular proteins. *Protein Eng.* **6**, 801-810.
 - [6] Holm, L. & Sander, C. (1993). Protein structure comparison by alignment of distance matrices. *J. Mol. Biol.* **233**, 123-138.
 - [7] Mirny, L. & Domany, E. (1996). Protein fold recognition and dynamics in the space of contact maps. *Proteins* **26**, 391-410.
 - [8] Vendruscolo, M., Kussell, E. & Domany, E. (1997). Recovery of Protein Structure from Contact Maps. *Fold. Des.* **2**, 295-306.
 - [9] Crippen, G. & Havel, T. F. (1988). *Distance geometry and molecular conformation*. Wiley, New York.
 - [10] Brünger, A. T., Adams, P. D. & Rice, L. M. (1997). New applications of simulated annealing in X-rays crystallography and solution NMR. *Curr. Op. Struct. Biol.* **5**, 325-336.
 - [11] Vendruscolo, M. & Domany, E. (1997). Efficient Dynamics in Contact Maps Space, in preparation.
 - [12] Miyazawa, S. & Jernigan, R. L. (1996). Residue-residue potentials with a favorable contact pair term and an unfavorable high packing density term, for simulation and threading. *J. Mol. Biol.* **256**, 623-644.
 - [13] Hinds, D. A. & Levitt, M. (1994). Exploring conformational space with a simple lattice model for

- protein structure. *J. Mol. Biol.* **243**, 668-682.
- [14] Thomas, P. D. & Dill, K. A. (1996). Statistical potential extracted from protein structures: How accurate they are? *J. Mol. Biol.* **257**, 457-469.
- [15] Jernigan, R. L. & Bahar, I. (1996). Structure derived potentials and protein simulations. *Curr. Opin. Struct. Biol.* **6**, 195-209.
- [16] Skolnick, J., Jaroszewski, L., Kolinski, A. & Godzik, A. (1997). Derivation and testing of pair potentials for protein folding. When is the quasi-chemical approximation correct?. *Protein Sci.* **6**, 676-688.
- [17] Lemer, C. M. -R., Rooman, M. J. & Wodak, S. J. (1995). Protein structure prediction by threading methods: Evaluation of current techniques. *Proteins* **23**, 337-355.
- [18] Maiorov, M. N. & Crippen, G. M. (1992). Contact potential that recognizes the correct folding of globular proteins. *J. Mol. Biol.* **227**, 876-888.
- [19] Goldstein, R. A., Luthey-Shulten, Z. A. & Wolynes, P. G. (1992). Protein tertiary structure recognition using optimized Hamiltonians with local interactions. *Proc. Natl. Acad. Sci. U.S.A.* **89**, 9029-9033.
- [20] Hao, M.-H. & Scheraga, A. (1996). How optimization of potential functions affects protein folding. *Proc. Natl. Acad. Sci. USA* **93**, 4984-4989.
- [21] Hao, M.-H. & Scheraga, A. (1996). Optimizing Potential Functions for Protein Folding. *J. Phys. Chem* **100**, 14540-14548.
- [22] Mirny, L. A. & Shakhnovich, E. I. (1996). How to derive a protein folding potential? A new approach to an old problem. *J. Mol. Biol.* **264**, 1164-1179.
- [23] Deutsch, J. M. & Kurosky, T. (1997). Design of force fields from data at finite temperature. *Phys. Rev. E* **56**, 4553-4557.
- [24] Rosenblatt, F. (1962). Principles of neurodynamics. Spartan books, New York.
- [25] Minsky, M. L. & Papert, S. A. (1969). Perceptrons. MIT press, Cambridge MA.
- [26] Cover, T. (1965). Geometrical and statistical properties of systems of linear inequalities with applications in pattern recognition. *IEEE Trans. Elect. Comput.* **14**, 326.
- [27] Gardner, E. (1988). The space of interactions in neural networks models. *J. Phys. A* **21**, 257.
- [28] Nabutovski, D. & Domany, E. (1991). Learning the Unlearnable. *Neural Computation* **3**, 604-616.
- [29] Vendruscolo, M., Domany, E., Subramanian, B. & Lebowitz, J. (1997). Statistical Properties of Physical Contact Maps, in preparation.
- [30] D. Fisher, D. Rice, Bowie J. U. & D. Eisenberg. (1996). Assigning amino acid sequences to 3-dimensional protein folds. *FASEB J.* **10**, 126-136.
- [31] Finkelstein, A. V. (1997). Protein structure: what is possible to predict now? *Curr. Op. Struct. Biol.* **7**, 60-71.
- [32] Najmanovich, R., Vendruscolo, M. & Domany, E. (1997). Learning a Protein Folding Potential for Threading, in preparation.
- [33] Wilson, C. & Doniach, S. (1989). A Computer Model of Dynamically Simulate Protein Folding: Studies with Crambin. *Proteins* **6**, 193-109.
- [34] Kolinski, A. & Skolnick, J. (1994). Monte Carlo Simulations of Protein Folding. II. Application to Protein A, ROP, and Crambin. *Proteins* **18**, 353-366.
- [35] Šali, A., Shakhnovich, E. I. & Karplus, M. (1994). Kinetics of protein folding. *J. Mol. Biol.* **235**, 1614-1636.
- [36] Teeter, M. M., Roe, S. M. & Heo, N. H. (1993). Atomic resolution (0.83 Angstroms) crystal structure of the hydrophobic crambin at 130 K. *J. Mol. Biol.* **230**, 292.
- [37] Lau, K. F. & Dill, K. A. (1989). A lattice statistical mechanics model of the conformational and sequence spaces of proteins. *Macromolecules* **22**, 3986-3997.